Available online at www.sciencedirect.com
ScienceDirect
Nuclear Physics B Proceedings Supplement 00 (2013) 1–6
Nuclear Physics B Proceedings Supplement

The Mu3e Experiment

Niklaus Berger for the Mu3e Collaboration

Physikalisches Institut, Heidelberg University

Abstract

The Mu3e experiment is designed to search for charged lepton flavour violation in the process $\mu^+ \to e^+e^-e^+$ with a branching ratio sensitivity of 10^{-16}. This requires a detector capable of coping with rates of up to $2 \cdot 10^9$ muons/s whilst being able to reduce backgrounds from accidental coincidences and the process $\mu^+ \to e^+e^-e^+\bar{\nu}_\mu\nu_e$ to below the 10^{-16} level. The use of 50 μm thin high-voltage monolithic active pixel sensors in conjunction with an innovative tracking concept provide the momentum and position resolution necessary, whilst the timing resolution is provided by a combination of scintillating fibres and tiles. The recently approved Mu3e experiment will be located at the Paul Scherrer Institute in Switzerland and is currently preparing for detector construction.

Keywords: Charged lepton flavour violation, Pixel Sensors, Muon Beams

1. Motivation

The discovery of neutrino oscillations has revealed that lepton flavour is not a conserved quantum number. Despite of a long history of searches (see e.g. [1, 2, 3] for reviews), no flavour violation has ever been observed in the charged lepton sector; these non-observations being one of the observational pillars on which the Standard Model (SM) of particle physics is built. If neutrino mixing in loops (see Figure 1, a)) are the only mechanism for charged lepton flavour violation (CLFV), the branching fractions for muons will indeed be suppressed to unobservable levels of $O(10^{-54})$. Many models predicting physics beyond the standard model (BSM) on the other hand lead to much larger CLFV branching fractions and are often strongly constrained by the existing experimental limits. See Figure 1 b) for an example involving supersymmetric particles and Figure 1 c) for a possible tree-level exchange of a heavy intermediary.

CLFV is being searched for mostly in the decays of muons and taus; whilst the taus have the advantage of a higher mass, leading to less suppression for most BSM effects, muons can be produced in much larger quantities (see section 3), leading to better sensitivities for many models. In the case of muons, the processes under study are the decay $\mu^+ \to e^+\gamma$, the conversion of a muon to an electron in the field of a nucleus and the process $\mu^+ \to e^+e^-e^+$; an overview of the experimental status for these three processes is given in Table 1.

The Mu3e experiment [9] is designed to search for $\mu^+ \to e^+e^-e^+$ with a branching ratio sensitivity of $< 10^{-16}$, an improvement by four orders of magnitude over the current limit. These proceedings will outline the challenges on the way to this sensitivity and discuss recent advances in beam and detector technology allowing to tackle these challenges.

2. Challenges

Reaching a branching ratio sensitivity of $< 10^{-16}$ in a reasonable running time requires a muon stop rate of about $2 \cdot 10^9$ s^{-1}; more than an order of magnitude more than what the πE5 beam line at PSI, the currently most intense source of muons for particle physics, is providing. The detector has to be capable of operating at these rates and detecting the signal process, namely two positrons and an electron from a common point in space and time with the four-momenta adding to that of a

Process	$\mu^+ \to e^+\gamma$	Muon conversion	$\mu^+ \to e^+e^-e^+$
Kinematics	2-body decay Monoenergetic e^+ and γ Back-to-back	Quasi 2-body decay Monoenergetic e^+ Single particle detected	3-body decay Invariant mass constraint Zero total momentum
Background	Accidental background	Decay in orbit Beam related backgrounds (π, $\bar{p}$) Cosmics	Radiative decay with internal conversion Accidental Background
Preferred beam	Continuous	Pulsed	Continuous
Best limit	$5.7 \cdot 10^{-13}$ MEG 2013 [4]	$7 \cdot 10^{-13}$ (Gold nuclei) SINDRUM II 2006 [5]	$1 \cdot 10^{-12}$ SINDRUM 1988 [6]
Planned experiments	MEG Upgrade [7] at PSI	Mu2e at Fermilab [8] DeeMe [10] and COMET [11] at J-PARC	Mu3e at PSI [9]
Planned single event sensitivity	$2 \cdot 10^{-14}$	Mu2e: $5.6 \cdot 10^{-17}$ DeeMe: $1 \cdot 10^{-14}$ COMET: $3 \cdot 10^{-17}$	$7 \cdot 10^{-17}$

Table 1: Comparison of muon CLFV experiments.

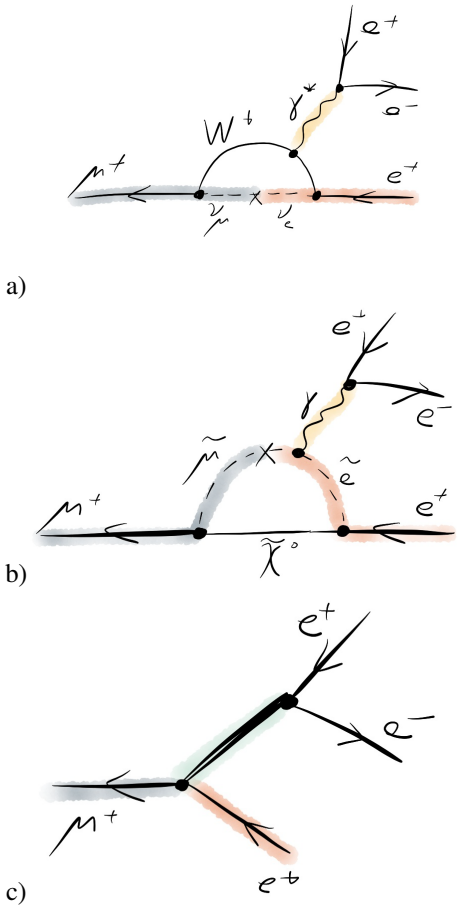

Figure 1: Diagrams for the process $\mu^+ \to e^+e^-e^+$ occurring via a) neutrino oscillations in the loop via b) supersymmetric particles in the loop or c) on tree level, via the exchange of a heavy intermediary (e.g. a Z' boson).

muon at rest. At the same time, backgrounds have to be reduced to below the 10^{-16} level. The main sources of background are on one hand accidental coincidences of positrons from the normal (Michel) muon decays combined with an electron from photon conversion, Bhabha scattering, mis-reconstruction etc.; this *accidental background* can be controlled with an excellent vertex, timing and momentum resolution. On the other hand, there is the radiative muon decay with internal conversion $\mu^+ \to e^+e^-e^+\bar{\nu}_\mu\nu_e$, which is indistinguishable from the signal except for the missing momentum carried away by the neutrinos. This *internal conversion background* can only be suppressed via a very precise momentum measurement.

The requirement of an excellent momentum measurement at very high rates drives the detector design; for the low momentum electrons and positrons[1], multiple coulomb scattering in detector material is dominating the momentum resolution. It is thus crucial to reduce the amount of material to an absolute minimum, whilst retaining a high rate capability and position and timing resolution. These challenges can be addressed with novel thin silicon pixel sensors and fast scintillating fibres and tiles, as described in section 4.

3. Muon Beams at PSI

The Paul Scherrer Institute (PSI) in Switzerland operates the most intense proton beam in the world with up to 2.3 mA of 590 MeV/c protons with 50 MHz repetition frequency. This beam is used to produce pions (and consequently muons) in two graphite production

[1] In the following, the term electron will be used to imply both charges.

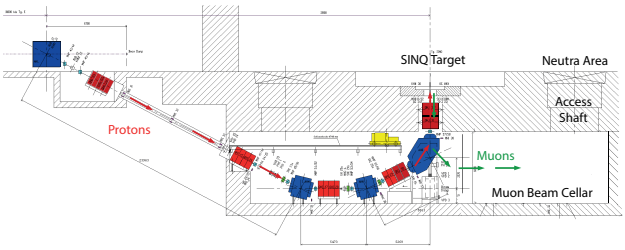

Figure 2: Schematic view of the proposed high intensity muon beam line at PSI.

targets. The πE5 beam line, home of the MEG experiment, provides up to 10^8 muons/s in a narrow momentum range around 29 MeV/c (surface muons), which can easily be stopped in a thin target. The high repetition rate combined with the long muon lifetime leads to continuous muon decays, ideal for experiments where accidental overlaps of several muon decays are an important source of background.

Most of the beam power at PSI ends up in the spallation target of the SINQ neutron source; besides neutrons, also very large numbers of pions are produced in that target. Capturing the muons from these pion decays could deliver up to 10^{10} muons/s to a new *High Intensity Muon Beam Line* (HiMB), a proposal which is currently under detailed study at PSI. This beam line, which would not be available before 2017, is a requirement for reaching the target sensitivity of the Mu3e experiment.

4. Detector Design

4.1. Pixel Sensors

The high rates expected in the Mu3e experiment preclude the use of gas detectors, where both space charge and ageing effects are of concern. On the other hand, hybrid silicon pixel sensors as employed e.g. in the ATLAS and CMS experiments put too much material into the path of the decay electrons. Monolithic active pixel sensors (MAPS, [13, 14]) can be thinned to less than 50 μm, but charge collection via diffusion makes them too slow for use in the Mu3e experiment. High-Voltage monolithic active pixel sensors (HV-MAPS [12, 15, 16, 17]) combine the advantages of MAPS with a "high" voltage of up to 90 V which is applied between the substrate and deep n-wells containing the transistors, see Figure 3. This voltage leads to fast ($\mathcal{O}$(1 ns)) charge collection via drift.

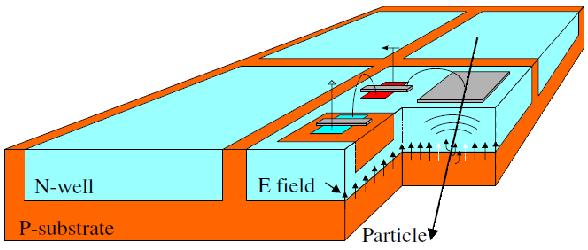

Figure 3: Schematic view of a HV-MAPS sensor. From [12].

The availability of analogue and digital logic in the sensor allows for an implementation of amplification, discrimination and a zero suppressing read-out logic; the sensor output consists of addresses and timestamps for the hit pixels and is sent over a fast low-voltage differential signalling link.

A series of HV-MAPS prototypes, the MUPIX chips, have been produced for Mu3e and tested in the lab using radioactive sources, LEDs and lasers as well as in test beam measurements [17, 18, 19]. With efficiencies above 99%, a signal-to-noise ratio above 20, spatial resolution given by the pixel size of 80 μm and a time resolution below 20 ns, these prototypes fulfil all the requirements of Mu3e; no degradation of performance has been observed in samples thinned to $\approx$ 90 μm.

4.2. Mechanics and Cooling

50 μm thin active pixel sensors are not self supporting and, in the case of the MUPIX chips, produce about 150 mW/cm^2 of heat. The support structure and cooling should however add as little material as possible. We have built structures consisting of a 25 μm thick Kapton® frame, another layer of 25 μm Kapton® foil representing the flexible printed circuit used to connect signals and power to the chips and thin glass plates representing the chips, see Figure 4. These structures are surprisingly sturdy, self-supporting over at least the 36 cm required for the detector and have a material budget (including the silicon) of less than a permille of a radiation length.

The detector will be cooled by gaseous helium, as this adds the smallest amount of material. The required flow rates of several meters per second pose a challenge for the very light mechanics; the cooling set-up is currently being tested using a full-size heatable mock-up of the detector.

4.3. Detector Geometry

The muon beam will be stopped in a hollow double cone target made of thin aluminium; the large target area helps in spreading out decay vertices and thus reducing

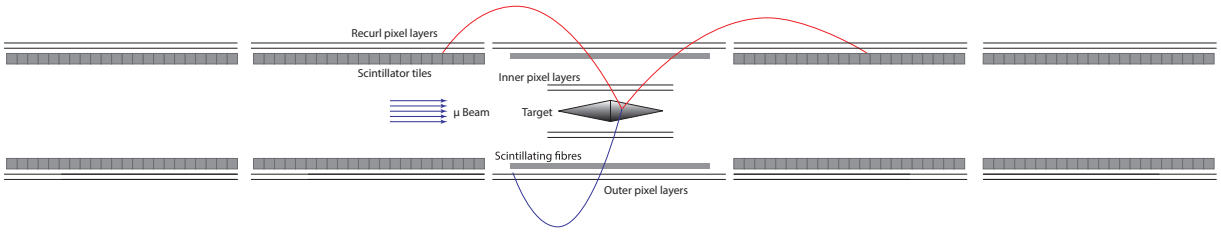

Figure 7: Schematic view of the detector geometry

Figure 4: Prototype of the inner detector layers built from Kapton® foil and thin glass plates representing the HV-MAPS sensors.

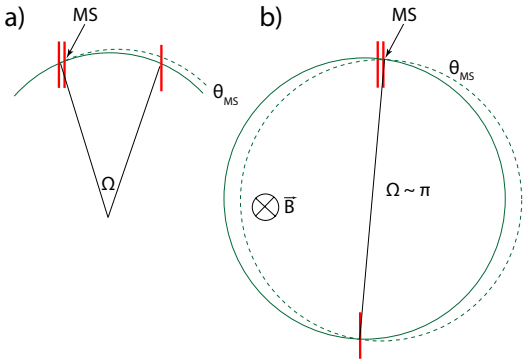

Figure 5: Effect of multiple scattering on the track momentum resolution, a) for an arbitrary lever arm Ω, b) for a lever arm of π.

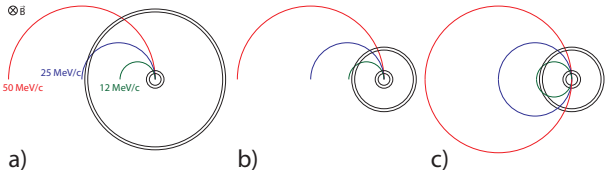

Figure 6: Detector geometries and momenta; a) optimal bending angle for 25 MeV/c electrons; b) acceptance down to 12 MeV/c; c) use of re-curling tracks for a combination of large bending angles and good acceptance.

accidental background. The rest of the detector geometry is optimized for the best possible momentum resolution.

In a multiple scattering dominated environment (i.e. if the effects of multiple scattering are large compared to the intrinsic detector resolution) the momentum resolution δp in a given magnetic field is

$$\delta p \propto \frac{\theta_{MS}}{\Omega}$$

with θ_{MS} the expected scattering angle and Ω the bending angle or lever arm, see Figure 5 a). For a bending angle of π, the effects of multiple scattering vanish to first order, see Figure 5 b). Thus, besides minimizing the amount of material (and thus the scattering angle θ_{MS}), a large lever arm is desirable. In muon decays, the electron momenta range from half the muon mass down to almost zero; the Mu3e experiment should be sensitive to transverse momenta above $\approx$ 12 MeV/c. In a conventional barrel-like detector, there is a trade-off between bending angle for high momentum tracks and acceptance for low momentum tracks, see Figure 6 a) and b). This can be circumvented by using re-curling tracks and thus measuring at large bending angles over the complete momentum range, see Figure 6 c). In order to retain a high acceptance for recurling tracks also in the forward and backward regions of the detector, a long tube design, see Figure 7, is used. The main contribution to the momentum measurement comes from the long arc in the helium outside the detector, which allows

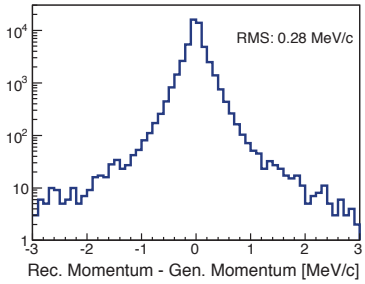

Figure 9: Simulated track momentum resolution for single tracks with a Michel-spectrum momentum distribution.

us to place timing detector between the inner and outer tracking stations.

4.4. Timing Detectors

In the central region, three layers of 250 μm scintillating fibres read out by arrays of silicon photomultipliers (SiPMs) give a timing resolution of about 1 ns, whilst inside the re-curl extensions, after which the tracks are no longer needed, scintillator tiles of 0.5 cm thickness coupled to SiPMs provide a timing resolution around 100 ps. The performance of the tile system has been demonstrated in test beam measurements and already fulfils the specifications.

4.5. Data Acquisition and Trigger

The complete Mu3e detector will have almost 300 million pixels and several thousand fibres and tiles. At the target rate of $2 \cdot 10^9$ muons/s, it will produce about 1 Tbit/s of zero suppressed data. We intend to read out all these data over optical links without a trigger, forward it to a farm of about 50 PCs with powerful graphics processing units (GPUs), reconstruct all the tracks and search for signal like topologies; the farm output data rate should be less than 100 MB/s. Due to the recurling tracks, the reconstruction problem is highly non-local, thus the complete detector information for a particular time slice has to be available on a particular farm PC. The sorting of the data from the position-sorted detector output to the time-sorted farm input is achieved with a switching network of FPGAs and optical links, see Figure 8.

4.6. Detector Performance

The detector performance is simulated both in a full, Geant4 [20, 21] based simulation and a simplified simulation for tracking studies with multiple scattering as the only detector effect on tracks. In both cases, we find a momentum resolution for tracks with a Michel spectrum

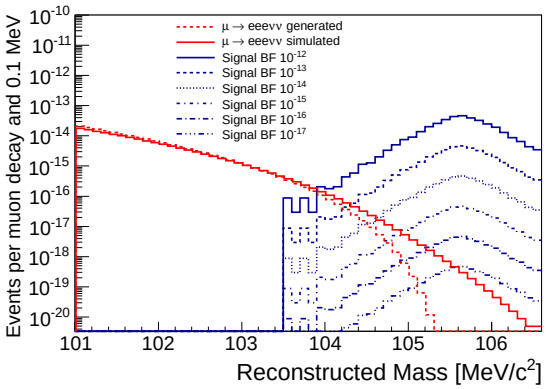

Figure 10: Simulation of the reconstructed three-particle mass for the internal conversion background superimposed with a $\mu^+ \to e^+e^-e^+$ signal (assuming a phase-space distribution of the electrons) at various strengths.

of about 300 keV/c over most of the detector acceptance and momentum range, see Figure 9. This, combined with a vertex resolution of $\approx$ 200 μm [22] in turn allows for an invariant three-particle mass reconstruction precise enough to separate the signal from the internal conversion tail to branching fractions below 10^{-16}, see Figure 10.

5. Outlook

The Mu3e experiment was approved by the PSI research committee in early 2013. Currently a vigorous research and development program with extensive test beam measurements of all subsystems is ongoing at all involved institutes. Detector construction and magnet procurement will start in 2014 and we hope for first measurements with the central part of the detector in 2016. After 2017, the high intensity muon beam line should become available, allowing for a push towards a sensitivity of 10^{-16} at the end of this decade.

Appendix A. Acknowledgments

The work of the author for the Mu3e experiment is generously supported by the *Deutsche Forschungsgemeinschaft* through an Emmy-Noether grant.

References

[1] Y. Kuno, Y. Okada, Muon decay and physics beyond the standard model, Rev. Mod. Phys. 73 (2001) 151–202. arXiv:hep-ph/9909265.

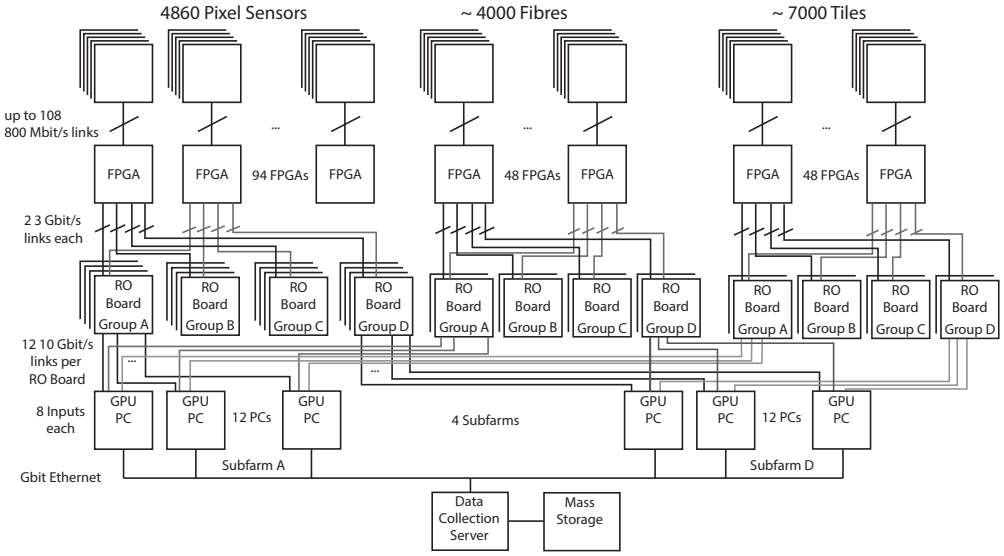

Figure 8: The Mu3e readout scheme.

[2] W. J. Marciano, T. Mori, J. M. Roney, Charged Lepton Flavor Violation Experiments, Ann.Rev.Nucl.Part.Sci. 58 (2008) 315–341. doi:10.1146/annurev.nucl.58.110707.171126.

[3] A. de Gouvea, P. Vogel, Lepton Flavor and Number Conservation, and Physics Beyond the Standard Model, Prog.Part.Nucl.Phys. 71 (2013) 75–92. arXiv:1303.4097, doi:10.1016/j.ppnp.2013.03.006.

[4] J. Adam, et al., New constraint on the existence of the $\mu^+ \to e^+\gamma$ decay, Phys. Rev. Lett. 110 (2013) 201801. doi:10.1103/PhysRevLett.110.201801.

[5] W. H. Bertl, et al., A Search for muon to electron conversion in muonic gold, Eur.Phys.J. C47 (2006) 337–346. doi:10.1140/epjc/s2006-02582-x.

[6] U. Bellgardt, et al., Search for the Decay $\mu^+ \longrightarrow e^+e^+e^-$, Nucl.Phys. B299 (1988) 1. doi:10.1016/0550-3213(88)90462-2.

[7] A. Baldini, F. Cei, C. Cerri, S. Dussoni, L. Galli, et al., MEG Upgrade Proposal arXiv:1301.7225.

[8] R. Abrams, et al., Mu2e Conceptual Design Report arXiv:1211.7019.

[9] A. Blondel, et al., Research Proposal for an Experiment to Search for the Decay $\mu \to eee$ arXiv:1301.6113.

[10] M. Aoki, An experimental search for muon-electron conversion in nuclear field at sensitivity of 10^{-14} with a pulsed proton beam, AIP Conf.Proc. 1441 (2012) 599–601. doi:10.1063/1.3700628.

[11] Y. Cui, et al., Conceptual design report for experimental search for lepton flavor violating μ^- - e^- conversion at sensitivity of 10^{-16} with a slow-extracted bunched proton beam (COMET).

[12] I. Peric, A novel monolithic pixelated particle detector implemented in high-voltage CMOS technology, Nucl.Instrum.Meth. A582 (2007) 876–885. doi:10.1016/j.nima.2007.07.115.

[13] M. Winter, Achievements and perspectives of cmos pixel sensors for charged particle tracking, Nucl. Instr. Meth. A 623 (1) (2010) 192 – 194, 1st International Conference on Technology and Instrumentation in Particle Physics. doi:DOI: 10.1016/j.nima.2010.02.192.

[14] J. Baudot, A. Besson, G. Claus, W. Dulinski, A. Dorokhov, M. Goffe, C. Hu-Guo, L. Molnar, X. Sanchez-Castro, S. Senyukov, M. Winter, Optimization of CMOS pixel sensors for high performance vertexing and tracking, Nucl. Instr. Meth. A. doi:http://dx.doi.org/10.1016/j.nima.2013.06.101.

[15] I. Peric, C. Takacs, Large monolithic particle pixel-detector in high-voltage CMOS technology, Nucl. Instrum. Meth. A624 (2) (2010) 504 – 508, new Developments in Radiation Detectors - "Proceedings of the 11th European Symposium on Semiconductor Detectors, 11th European Symposium on Semiconductor Detectors". doi:DOI: 10.1016/j.nima.2010.03.161.

[16] I. Peric, C. Kreidl, P. Fischer, Particle pixel detectors in high-voltage CMOS technology–New achievements, Nucl. Instrum. Meth. A650, Issue 1 (2010) 158–162. doi:10.1016/j.nima.2010.11.090.

[17] I. Peric, et al., High-voltage pixel detectors in commercial CMOS technologies for ATLAS, CLIC and Mu3e experiments, Nucl. Instrum. Meth. A, In Press. doi:http://dx.doi.org/10.1016/j.nima.2013.05.006.

[18] A.-K. Perrevoort, Characterisation of High Voltage Monolithic Active Pixel Sensors for the Mu3e Experiment, Master thesis, Heidelberg University (2012).

[19] H. Augustin, Charakterisierung von hv-maps, Bachelor thesis, Heidelberg University (2012).

[20] S. Agostinelli, et al., Geant4–a simulation toolkit, Nucl. Instr. Meth. A 506 (3) (2003) 250 – 303. doi:DOI: 10.1016/S0168-9002(03)01368-8.

[21] J. Allison, K. Amako, J. Apostolakis, H. Araujo, P. Dubois, et al., Geant4 developments and applications, IEEE Trans. Nucl. Sci. 53 (2006) 270. doi:10.1109/TNS.2006.869826.

[22] S. Schenk, A Vertex Fit for Low Momentum Particles in a Solenoidal Magnetic Field with Multiple Scattering, Master's thesis, Heidelberg University (2013).